1-22-2001

SiGe/Si THz laser based on transitions between inverted mass light-hole and heavy-hole subbands

L. Friedman
Air Force Research Laboratory, Hanscom Air Force Base

Greg Sun
University of Massachusetts Boston, greg.sun@umb.edu

Richard A. Soref
Air Force Research Laboratory, Hanscom Air Force Base

SiGe/Si THz laser based on transitions between inverted mass light-hole and heavy-hole subbands

L. Friedman, G. Sun, and R. A. Soref

Citation: Appl. Phys. Lett. **78**, 401 (2001); doi: 10.1063/1.1341221
View online: http://dx.doi.org/10.1063/1.1341221
View Table of Contents: http://apl.aip.org/resource/1/APPLAB/v78/i4
Published by the American Institute of Physics.

SiGe/Si THz laser based on transitions between inverted mass light-hole and heavy-hole subbands

L. Friedman
Sensors Directorate, Air Force Research Laboratory, Hanscom AFB, Massachusetts 01731

G. Sun[a)]
Department of Physics, University of Massachusetts at Boston, Boston, Massachusetts 02125

R. A. Soref
Sensors Directorate, Air Force Research Laboratory, Hanscom AFB, Massachusetts 01731

(Received 23 May 2000; accepted for publication 15 November 2000)

We have investigated a SiGe/Si quantum-well laser based on transitions between the light-hole and heavy-hole subbands. The lasing occurs in the region of **k** space where the dispersion of ground-state light-hole subband is so nonparabolic that its effective mass is inverted. This kind of lasing mechanism makes total population inversion between the two subbands unnecessary. The laser structure can be electrically pumped through tunneling in a quantum cascade scheme. Optical gain as high as 172/cm at the wavelength of 50 μm can be achieved at the temperature of liquid nitrogen, even when the population of the upper laser subband is 15% less than that of the lower subband. © *2001 American Institute of Physics.* [DOI: 10.1063/1.1341221]

The rapid advance of epitaxial growth techniques has made possible the investigation of many Si-based heterostructures appealing for optoelectronic applications, including Ge-Si, SiGeC/Si, Si/ZnS, Si/BeSeTe, Si/γ-Al_2O_3, Si/CeO_2, and Si/SiO_x.[1–4] We have previously studied some of these structures mainly for mid-to-near IR laser applications.[5,6] The focus of this investigation is on the feasibility of Si-based laser structures capable of THz emission for applications such as space-based communications. While there has been a previous attempt in achieving THz emission in the conduction band of III-V devices,[7] our approach is based on an earlier design of valence intersubband lasers with inverted light-hole effective mass proposed for the GaAs/AlGaAs quantum well (QW) system.[8] We have used an anti crossing between the heavy-hole 2 (HH2) and light-hole 1 (LH1) subbands in the SiGe/Si system to engineer a LH1 subband that is electron-like over a region of **k** space where LH1 and HH1 subbands have opposite curvature. These subbands, at their closest approach, have energy separation in the THz frequency range, and their diverging curves prevent self-absorption of photons emitted at the **k** valley.

We have calculated the in-plane dispersion of $Si_{1-x}Ge_x$/Si valence subband structures using the Kane model.[9] Because of the indirect nature of the Si and Ge band gaps, the conduction band (CB) is effectively decoupled from the valence band, so that the 8×8 Hamiltonian matrix in the $\mathbf{k}\cdot\mathbf{p}$ theory reduces to a 6×6 valence band matrix taking into account the coupling between HH, LH, and spin-orbit (SO) bands, as well as strain in the QWs. Several $Si_{1-x}Ge_x$/Si superlattices (SLs) have been investigated. In asymmetrically strained $Si_{1-x}Ge_x$/Si SLs grown on a Si substrate, flattening of the dispersion of the ground-state LH subband (LH1) was seen, but no inverted mass was found. However, we have found the symmetrically strained $Si_{1-x}Ge_x$/Si SL on a relaxed $Si_{1-y}Ge_y$ buffer layer is more promising for this type of laser. Si-based $Si_{1-y}Ge_y$ buffers with a wide range of composition ($0<y<1.0$) have been developed by the MIT group.[10] We have examined several cases of symmetrically strained $Si_{1-x}Ge_x$/Si SLs on a $Si_{1-y}Ge_y$ buffer, in which the in-plane tensile strain of the Si barriers was chosen equal and opposite to the in-plane compressive strain of the $Si_{1-x}Ge_x$ QWs. We further determined the buffer composition y so that the lattice parameter of the buffer was equal to the average in-plane lattice constant of the free standing $Si_{1-x}Ge_x$/Si SL, thus ensuring coherent SL strain. Several such constructed SLs showed inverted mass in the LH1 subband, among which we have chosen the SL consisting of 90 Å $Si_{0.7}Ge_{0.3}$ QWs and 50 Å Si barriers on a (100) $Si_{0.81}Ge_{0.19}$ buffer for investigating the feasibility of lasing because this heterostructure produces not only the inverted mass in the LH1 subband, but also an energy separation between subbands HH1 and LH1 in the THz frequency range. The in-plane dispersion in the (110) direction of this symmetrically strained 90 Å/50 Å $Si_{0.7}Ge_{0.3}$/Si SL is shown in Fig. 1 of Ref. 11. The band offsets at $\mathbf{k}=0$ are $V_{hh}=216.5$ meV, $V_{lh}=108.4$ meV, and the in-plane lattice constant $a_o=5.474$ Å. The LH1 subband has an energy valley 2 meV deep at $k_x=k_y=0.014\,\text{Å}^{-1}$, which extends from 0 to $0.025\,\text{Å}^{-1}$. The presence of bound subbands lying higher in hole energy than LH1 does not have much influence on laser operation, as discussed below. Figure 1 presents a detailed view of the in-plane dispersions of three lowest-lying subbands. The numericals 1, 2, 3, 4, indicate how this inverted mass intersubband laser mimics the operation of a conventional band-to-band laser.[11] The upper-state lifetime is long because the intersubband transition energy is below that of optical phonons, allowing only much weaker acoustic phonon scattering between the two different bands. Recently,[11] we have calculated the upper-state lifetime, τ_a, due to the acoustic phonon scattering and find that $\tau_a=2.0$ ns, which is

[a)]Electronic mail: gsun@cs.umb.edu

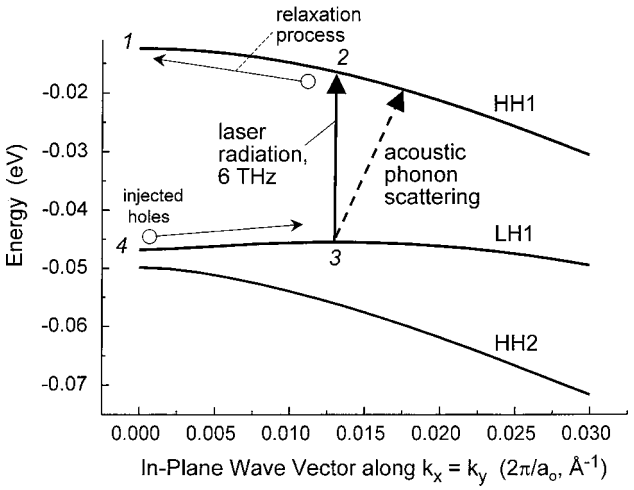

FIG. 1. A detailed view of the in-plane dispersions of three lowest-lying subbands showing the laser operating process.

much longer than the typical lifetime of 1 ps when it is between the subbands of the same type, say, HH to HH or CB to CB.

The proposed laser structure is a highly simplified version of the quantum cascade that resembles the scheme of Kazarinov and Suris.[12] As shown in Fig. 2, holes from the lower subband HH1 in the previous lasing period tunnel through the Si barrier to the upper subband LH1 in the next period. The tunneling time, τ_t, between subbands HH1 and LH1 can be controlled by tuning the width of the Si barrier separating the $Si_{0.7}Ge_{0.3}$ QWs. A competing process of acoustic phonon scattering (Fig. 2) leaks a small fraction of holes directly to the lower subband HH1 in the next laser period without contributing to the lasing process.

Since the intrasubband process is significantly faster than the intersubband process, it is reasonable to assume that the hole distribution within each of the involved subbands has reached quasiequilibrium during the lasing operation and therefore can be described by the quasi-Fermi levels (E_{Fl}, E_{Fh}) for LH and HH subbands respectively. The total hole population N injected by the pumping current is distributed between subbands HH1 (N_h) and LH1 (N_l) as

$$N = N_h(E_{\mathrm{Fh}}) + N_l(E_{\mathrm{Fl}}). \tag{1}$$

A rate equation can be established for the population of subband LH1

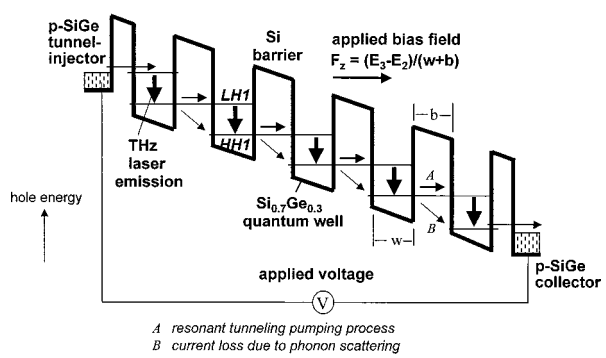

FIG. 2. A schematic of the inverted-mass intersubband laser with a quantum cascade scheme.

$$\frac{\partial N_l}{\partial t} = \frac{N_h}{\tau_t} - \frac{N_l}{\tau_a} - \frac{N_l}{\tau_s} \tag{2}$$

taking into account contributions from carrier tunneling, acoustic phonon scattering, and spontaneous emissions. The carrier-carrier scattering is not expected to be strong in this type of laser and is therefore neglected because there is little overlap between the two different LH and HH Bloch wave functions. Their subbands are quite nonparabolic to each other, which does not allow both energy and momentum to be conserved in the carrier-carrier scattering event. The lifetime $\tau_a = 2.0$ ns at 77K according to our calculation. The tunneling time τ_t largely determined by the Si-barrier width is not calculated in this study, but rather used as a tuning parameter to demonstrate the advantage of lasing without the total population inversion between the two subbands. The spontaneous emission rate is given as the inverse of the radiative lifetime

$$\frac{1}{\tau_s} = \frac{\tilde{n} e^2 E}{3\pi^2 \epsilon_o m_o^2 c^3 \hbar^2} |M_p(E)|^2, \tag{3}$$

where $\hbar$ is the Planck constant, m_o and e are the free-electron mass and charge, ϵ_o and c are the permittivity and light velocity in vacuum, $\tilde{n}$ is the index of refraction, E and $M_p(E)$ are the transition energy and momentum matrix element between subbands LH1 and HH1, respectively. The induced transition rate is not included in Eq. (2) because the rate equation was established below the lasing threshold.

A steady-state distribution can be obtained by setting Eq. (2) to be zero, then solved simultaneously with Eq. (1). Solving both equations self-consistently, we are able to obtain quasi-Fermi levels for subbands LH1 and HH1 with given total hole concentration N and tunneling time τ_t. The resulting quasi-Fermi levels are then used in the following expression for optical gain:

$$\gamma(E) = \frac{\pi e^2 \hbar \eta}{m_o^2 E} |M_p(E)|^2 \rho_r(E) [f_l(E_l) - f_h(E_h)]|_{E_l - E_h = E}, \tag{4}$$

where $\eta = 1/\epsilon_o c \tilde{n} = 377\Omega/\tilde{n}$ is the impedance of the medium, $\rho_r(E)$ is the reduced density of states for the LH-HH transition, and $f_l(E_l)$ and $f_h(E_h)$ are the Fermi-Dirac distribution for holes in subbands LH1 and HH1, respectively. Regarding the momentum matrix element M_p, the radiative selection rule is that the LH1-HH1 transition is strongly allowed for THz light polarized in the XY growth plane. This polarization is suitable for vertical-cavity surface-emitting lasers.

The optical gain of Eq. (4) has been evaluated for the LH1-to-HH1 transition at the local maximum of the LH1 subband as shown in Fig. 1. The transition energy is 25 meV, corresponding to a wavelength of 50 μm at 6 THz. The result is shown in Fig. 3 as a function of the tunneling time τ_t for several densities of hole population in the $1\times10^{17}\sim1\times10^{18}/\mathrm{cm}^3$ range. Positive optical gain ranging from $\sim100/\mathrm{cm}$ to over 1000/cm is obtained when the tunneling time is shorter than that of the upper laser state, $\tau_t < \tau_a = 2.0$ ns. This is obviously expected because it corresponds to the case of total population inversion between the two

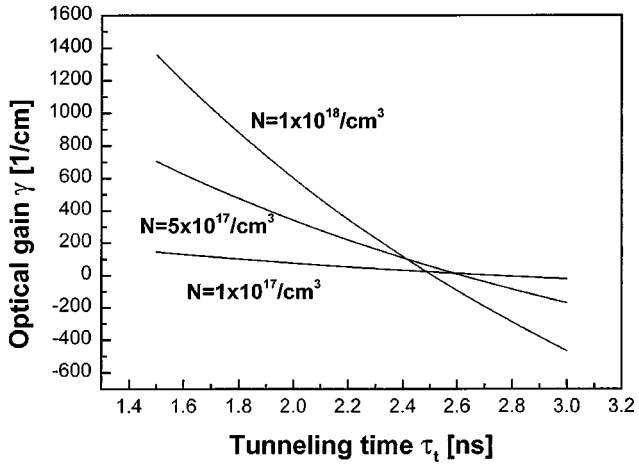

FIG. 3. Optical gain as a function of the tunneling time τ_t for hole densities N_l+N_h in the range of $1\times10^{17}/\mathrm{cm}^3$ $1\times10^{18}/\mathrm{cm}^3$.

subbands LH1 and HH1, $N_l>N_h$, which is not the focus of our investigation. In order to demonstrate the advantage of inverted mass lasing, our attention is directed toward the feasibility of optical gain without total inversion, $N_l<N_h$ by allowing the tunneling time to be longer than that of the upper laser state, $\tau_t>\tau_a$. It can be seen in Fig. 3 that fairly large optical gain on the order of a few 100/cm can be achieved even when $\tau_t>\tau_a=2.0\,\mathrm{ns}$. It is also shown in Fig. 3 that optical gain for larger density of total hole population tends to decrease faster as a function of tunneling time. For $N=1\times10^{17}/\mathrm{cm}^3$, the optical gain remains positive, $\gamma>0$ until $\tau_t=2.73\,\mathrm{ns}$ corresponding to $N_l=0.73N_h$, for $N=5\times10^{17}/\mathrm{cm}^3$, $\gamma>0$ until $\tau_t=2.61\,\mathrm{ns}$ corresponding to $N_l=0.77N_h$, while for $N=1\times10^{18}/\mathrm{cm}^3$, $\gamma>0$ until $\tau_t=2.51\,\mathrm{ns}$ corresponding to $N_l=0.8N_h$. Figure 4 shows the optical gain γ as a function of the total hole population, N, for $\tau_t=2.35\,\mathrm{ns}$, corresponding to $N_l=0.85N_h$. The optical gain in Fig. 4 reaches a maximum of 172/cm at $N=10^{18}/\mathrm{cm}^3$. This gain is significantly larger than that measured in an 8.9 μm electron-injected GaAs/AlGaAs quantum cascade laser,[13] and will be large enough for lasing if the free-hole absorption coefficient within the laser cavity is kept below 100/cm.

At $\mathbf{k}=0$, the energy separation between LH1 and HH2 is 4 meV in Fig. 1. This spacing can be increased by QW engineering, but as the separation increases, the inverted-mass feature disappears. In Fig. 2, during strong pumping, some holes from HH1 will tunnel into HH2 (rather than LH1) of the next QW. However, this divided injection is a small effect because the downward subband curvature of HH2 as shown in Fig. 1 suppresses unwanted injection into HH2. In Fig. 2, most of the holes injected into LH1 make the vertical transition to HH1, but a small percentage of those holes, according to Fig. 1, will leak into HH2 of the next well by tunneling. However, at resonance, the state in HH2 has a much larger in-plane **k** vector than that in LH1, thus this tunneling rate is low and the excited state leakage is small. A strategy for inhibiting leakage is to complicate the Fig. 2 structure by inserting a chirped SL of SiGe/Si between each QW and barrier. Using the same SiGe composition, it is feasible to design the SL so that its lowest miniband faces HH1 and its minigap faces LH1 when biased as in Fig. 2. Self-absorption of emitted laser photons is not problematical. Absorption from the LH1 valley to HH2 is forbidden because the **k** vector and photon energy are not conserved simultaneously in that transition.

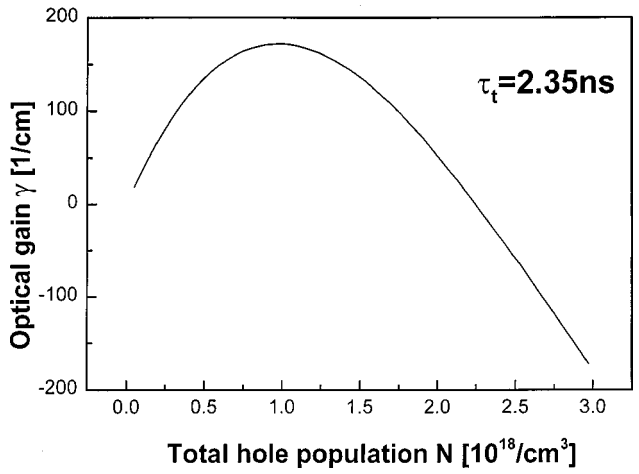

FIG. 4. Optical gain as a function of the total hole density N for $\tau_t=2.35\,\mathrm{ns}$, corresponding to $N_l=0.85N_h$ without total population inversion.

In summary, we have theoretically studied SiGe/Si intersubband lasers based on LH-HH transition in the region of inverted LH effective mass in **k** space. The active region of the particular laser structure under investigation is designed with simple single $Si_{0.7}Ge_{0.3}$ QWs separated by Si barriers on a Si substrate with a $Si_{0.81}Ge_{0.19}$ buffer. This buffer layer is chosen such that the wells and barriers in the laser structure are symmetrically strained. The lasing transition is determined to be at 50 μm wavelength, corresponding to 6 THz, and is designed to operate at the temperature of liquid nitrogen. The laser structure can be pumped electrically with a quantum cascade scheme where the holes tunnel through Si barriers from one lasing period to the next. The tunneling time can be controlled by the Si-barrier thickness and is used as a parameter in determining the hole population distribution between the two involved subbands LH1 and HH1. We have demonstrated that optical gain in excess of 100/cm can be achieved when no total population inversion is established between LH and HH subband, $N_l<N_h$. In particular, for $N_l=0.85N_h$, optical gain as high as 172/cm can be readily obtained.

[1] R. A. Soref, M. Atzmon, F. Shaapur, McD. Robinson, and R. Westhoff, Opt. Lett. **21**, 345 (1996).
[2] L. C. Lew YanVoon, L. R. Ram-Mohan, and R. A. Soref, Appl. Phys. Lett. **70**, 1837 (1997).
[3] L. T. Romano, R. D. Bringans, and W. P. Kirk, Phys. Rev. B **52**, 11201 (1995).
[4] J. Ding and R. Tsu, Appl. Phys. Lett. **71**, 2124 (1997).
[5] L. Friedman, R. A. Soref, G. Sun, and Y. Lu, IEEE J. Sel. Top. Quantum Electron. **4**, 1029 (1998).
[6] R. A. Soref, L. Friedman, L. C. Lew Yan Voon, L. R. Ram-Mohan, and G. Sun, J. Vac. Sci. Technol. B **16**, 1525 (1998).
[7] M. Rochat, J. Faist, M. Beck, U. Oesterle, and M. Ilegems, Appl. Phys. Lett. **73**, 3724 (1998).
[8] G. Sun, Y. Lu, and J. B. Khurgin, Appl. Phys. Lett. **72**, 1481 (1998).
[9] E. O. Kane, J. Phys. Chem. Solids **1**, 249 (1957).
[10] S. B. Samavedam, M. T. Currie, T. A. Langdo, S. M. Ting, and E. A. Fitzgerald, Mater. Res. Soc. Symp. Proc. **486**, 187 (1998).
[11] G. Sun, L. Friedman, and R. A. Soref, Phys. Rev. B **62**, 8114 (2000).
[12] R. F. Kazarinov and R. A. Suris, Sov. Phys. Semicond. **51**, 707 (1971).
[13] S. Barbieri, C. Sirtori, H. Page, M. Beck, J. Faist, and J. Nagle, IEEE J. Quantum Electron. **36**, 736 (2000).